

# Description of nuclei in the $A \sim 100$ mass region with the interacting boson model

M Böyükata<sup>1</sup>, P Van Isacker<sup>2</sup> and İ Uluer<sup>1</sup>

<sup>1</sup>Physics Department, Faculty of Science and Arts, University of Kırıkkale,  
71100 Kırıkkale, Turkey

<sup>2</sup>Grand Accélérateur National d'Ions Lourds, CEA/DSM-CNRS/IN2P3, B.P. 55027,  
F-14076 Caen Cedex 5, France

**Abstract.** Even-even nuclei in the  $A \sim 100$  mass region are investigated within the framework of the interacting boson model-1 (IBM-1). The study includes energy spectra and electric quadrupole transition properties of zirconium, molybdenum, ruthenium and palladium isotopes with neutron number  $N \geq 52$ . A global parametrization of the IBM-1 Hamiltonian is found leading to a description of about 300 collective levels in 30 nuclei with a root-mean-square deviation from the observed level energies of 120 keV. The importance of the  $d_{5/2}$  subshell closure at neutron number  $N = 56$  is pointed out. The geometric character of the nuclei can be visualized by plotting the potential energy surface  $V(\beta, \gamma)$  obtained from the IBM-1 Hamiltonian in the classical limit. The parametrization established on the basis of known elements is used to predict properties of the unknown, neutron-rich isotopes  $^{106}\text{Zr}$ ,  $^{112}\text{Mo}$ ,  $^{116}\text{Ru}$  and  $^{122}\text{Pd}$ .

PACS numbers: 21.60.Ev, 21.10.Re, 21.60.Fw

*Keywords:* nuclear level energies, E2 transitions, interacting boson model

## 1. Introduction

The production and use of radioactive beams is a rapidly developing new field in nuclear physics. Pioneering experiments are taking place, dedicated facilities are commissioned and new ones are planned. The primary aim of this research activity is the study of so-called exotic nuclei, that is, short-lived nuclei far removed from the line of stability because of an unusual ratio of numbers of neutrons  $N$  over protons  $Z$ . Parallel with the rapid developments of experimental techniques to observe exotic nuclei, there has been a surge in the interest in their theoretical description.

The main motivation for these studies is the possibility that wide variations in  $N/Z$  may have a profound influence on shell structure, which constitutes the basis of our understanding of nuclei. There exist currently two standard theoretical approaches for the description of exotic nuclei, namely energy density functional theory [1] and the nuclear shell model [2]. In this paper we explore the use of a third approach, namely the interacting boson model (IBM) of Arima and Iachello [3, 4, 5], to predict properties of exotic nuclei.

The IBM is a semi-microscopic model of nuclei, positioned intermediately between single-particle and collective models. The model contains a vibrational and a rotational limit (as well as one which can be considered as intermediate)—which connects well with the phenomenology of nuclei—and can be brought into relation with the nuclear shell model. In the original version of the IBM, applicable to even-even nuclei, the basic building blocks are  $s$  and  $d$  bosons with angular momenta  $L = 0$  and  $L = 2$ , respectively. The  $s$  and  $d$  bosons can be interpreted as correlated Cooper pairs formed by two nucleons in the valence shell coupled to angular momenta  $L = 0$  and  $L = 2$ . This interpretation constitutes the basis of the connection between the IBM and the nuclear shell model, and leads in a natural way to a version of the model where a distinction is made between neutron and proton bosons, the so-called IBM-2 [6].

If one restricts oneself to configurations that are symmetric in the neutron and proton bosons, the simplest version of the model arises, known as IBM-1. The standard IBM-1 Hamiltonian has 1 single-particle energy and 5 two-body interactions if only relative (excitation) energies are considered, increasing to  $2 + 7$  if absolute binding energies are included in the analysis. These coefficients enter as free parameters in the model and must be adjusted to the data. However, because of the connection with the nuclear shell model, the dependence of the energies and interactions on the number of valence neutrons and protons is known qualitatively [7]. The long-term aim of this work is to develop a systematic IBM-1 parametrization (that is, to determine the functional dependence of the various coefficients on the number of valence neutrons and protons) for entire regions of nuclei, and to do so on the basis of a fit to the data, guided by microscopic arguments. Once the appropriate functional dependence has been determined, it will be possible to make spectroscopic predictions by extrapolation to unknown regions of nuclei. The predictive power of this procedure will depend crucially on the counting of the valence nucleons and hence on the shell structure of nuclei and

its evolution in exotic regions.

The idea to use the IBM to extrapolate from known to unknown regions of the nuclear chart is not new. In fact, in the late 1970s and early 1980s, long before any talk of exotic nuclei, this technique was applied on many *isotope* series in the context of the IBM-2. For a review of the literature, see Iachello and Arima [8]. Occasionally also *isotone* series have been considered [9] and recently also a combination of *isobars* and *isotones* [10]. However, to our knowledge a comprehensive and systematic description with the IBM of entire *regions* of nuclei has not yet been tried. The closest related study is due to Casten *et al.* [11] who elaborated a multi-nucleus IBM-1 parametrization based on the  $N_\nu N_\pi$  scheme [12]. Our intention is to develop this idea further with more refined Hamiltonians that better reproduce observed nuclear properties. We also mention that our investigation has similar aims as those of the recent work of the Tokyo group [13], (*i.e.*, the use of the IBM in the description of exotic nuclei); in the latter studies the connection of the IBM with mean-field models is exploited to arrive at a suitable parametrization while here the long-term aim is to draw inspiration from its connection with the shell model.

In this paper we present a first calculation of this type and apply the IBM-1 to an entire region of the nuclear mass chart, namely the even–even Zr, Mo, Ru and Pd nuclei with  $A \sim 100$ . Section 2 gives a description of the parametrization of the Hamiltonian used. The application to the  $A \sim 100$  region is discussed in section 3. In the final section 4 the conclusions and outlook are presented. Preliminary versions of this work were presented in references [14, 15].

## 2. Parametrization of the Hamiltonian

The Hamiltonian used in this paper is of the form

$$\hat{H} = \epsilon \hat{n}_d + \kappa \hat{Q} \cdot \hat{Q} + \kappa' \hat{L} \cdot \hat{L} + \kappa'' \hat{P}_+ \cdot \hat{P}_- + \lambda \hat{n}_d^2, \quad (1)$$

where  $\hat{n}_d$ ,  $\hat{P}_+$ ,  $\hat{L}$  and  $\hat{Q}$  are the boson-number, pairing, angular momentum and quadrupole operators, defined as

$$\begin{aligned} \hat{n}_d &= \sqrt{5} [d^\dagger \times \tilde{d}]_0^{(0)}, \\ \hat{P}_+ &= [s^\dagger \times s^\dagger + \sqrt{5} d^\dagger \times d^\dagger]_0^{(0)}, \quad \hat{P}_- = (\hat{P}_+)^{\dagger}, \\ \hat{L}_\mu &= \sqrt{10} [d^\dagger \times \tilde{d}]_\mu^{(1)}, \\ \hat{Q}_\mu &= [d^\dagger \times \tilde{s} + s^\dagger \times \tilde{d}]_\mu^{(2)} + \chi [d^\dagger \times \tilde{d}]_\mu^{(2)}. \end{aligned} \quad (2)$$

Equation (1) defines an IBM-1 Hamiltonian in terms of the six parameters  $\epsilon$ ,  $\kappa$ ,  $\kappa'$ ,  $\kappa''$ ,  $\lambda$  and  $\chi$ . If one is interested in the properties of a single nucleus, this is a possible form of the most general Hamiltonian with the advantage that the first four terms have been used extensively in phenomenological fits to nuclear spectra [8]. The last term  $\hat{n}_d^2$  gives rise to a so-called ‘ $\tau$ -compression’ which increases the moment of inertia with increasing angular momentum (or with increasing  $d$ -boson seniority  $\tau$ ) [16]. In addition to measured energy spectra, also electric quadrupole transition rates are considered in

the fit. These are calculated in IBM-1 using the E2 operator  $\hat{T}_\mu(\text{E2}) = e_b \hat{Q}_\mu$  where  $e_b$  is the effective charge of a boson and with a quadrupole operator which is consistent with the one used in the Hamiltonian, following the consistent- $Q$  formalism (CQF) [17].

Although reasonable results are obtained with a constant Hamiltonian, they are considerably improved if parameters are allowed to vary with the number of nucleons in the valence shell, as suggested by the shell-model interpretation of the IBM-1. We propose here a dependence of the generic form

$$x = \sum_{ij} x_{ij} (f_\nu)^i (f_\pi)^j, \quad (3)$$

where  $x$  is a parameter of the Hamiltonian, that is,  $x = \epsilon, \kappa, \kappa', \kappa''$  or  $\lambda$ , and  $f_\rho$  is the fractional filling of the neutron ( $\rho = \nu$ ) or the proton ( $\rho = \pi$ ) valence shell, that is,  $f_\rho \equiv n_\rho / \Omega_\rho$  with  $n_\rho$  the number of valence neutrons or protons and  $\Omega_\rho$  the size of the corresponding valence shell. Note that in the parametrization (3) neutrons and protons are always counted as particles and never as holes. While microscopic arguments suggest a dependence on  $F_\rho \equiv \bar{n}_\rho / \Omega_\rho$  rather than on  $f_\rho$  (where  $\bar{n}_\rho$  is the number of particles or holes, whichever is smaller counted from the nearest closed shell), the latter parametrization has the drawback of yielding spectra that are symmetric around mid-shell. Since this particle-hole symmetry is broken in the nuclei considered here, especially in the Pd isotopes, we prefer the parametrization (3).

### 3. Application to the $A \sim 100$ region

In the present application to the  $A \sim 100$  region a linear dependence on the fractional fillings is assumed for the parameters  $\kappa, \kappa'$  and  $\lambda$  while  $\epsilon$  and  $\kappa''$  are kept constant. First, energy levels in the known nuclei  $^{100-104}\text{Zr}$ ,  $^{94-110}\text{Mo}$ ,  $^{98-114}\text{Ru}$  and  $^{102-120}\text{Pd}$  are selected and fitted with the IBM-1 Hamiltonian (1) by minimizing the root-mean-square (rms) deviation. In this first step an initial choice is made for  $\chi$ , and  $\epsilon, \kappa, \kappa', \kappa''$  and  $\lambda$  are fitted to the energy spectra of all nuclei considered in the fit with no dependence on the number of neutrons or protons. Next, the linear dependence on the fractional filling of the parameters  $\kappa, \kappa'$  and  $\lambda$  is determined again by minimizing the rms deviation. The minimization in this case involves 11 parameters, three for each coefficient in the Hamiltonian with a fractional-filling dependence together with  $\epsilon$  and  $\kappa''$ . Once the wave functions of all states have been determined in this unified fit, the E2 transition rates are fitted by adjusting the value of the boson effective charge  $e_b$  but keeping to the same value of  $\chi$ . Since  $B(\text{E2})$  properties depend rather strongly on  $\chi$ , it is at this point that it can be established whether its value is appropriate or not. The entire procedure is repeated for a new value of  $\chi$ , until a reasonable compromise is found between the results of the energy and E2 fits.

This procedure is illustrated in table 1. The rms deviations in the energies and  $B(\text{E2})$  values are quantified with following definitions:

$$\Delta(E) = \sqrt{\frac{1}{N_E} \sum_i (E_{\text{ex}}^i - E_{\text{th}}^i)^2},$$

**Table 1.** Root-mean-square deviations  $\Delta$  in the energies and  $B(E2)$  values as a function of the quadrupole parameter  $\chi$ .

$\chi$	-0.05	-0.1	-0.2	-0.3	-0.4	-0.6	-0.8	-1.0
$\Delta(E)$ (keV)	126	122	120	122	125	129	131	133
$\Delta_1(E2)$ ( $e^2b^2$ )	0.26	0.13	0.10	0.11	0.14	0.17	0.15	0.16
$\Delta_2(E2)$	3.44	2.29	2.02	2.12	2.34	2.54	2.20	2.21

**Table 2.** Parameters of the Hamiltonian (1) in units of keV.

$\epsilon$	$\kappa_{00}$	$\kappa_{10}$	$\kappa_{01}$	$\kappa'_{00}$	$\kappa'_{10}$	$\kappa'_{01}$	$\kappa''$	$\lambda_{00}$	$\lambda_{10}$	$\lambda_{01}$
695	-35.8	-72.4	47.9	18.3	12.8	-15.8	1.4	-115.9	-166.1	161.2

$$\Delta_1(E2) = \sqrt{\frac{1}{N_{E2}} \sum_i (B(E2)_{\text{ex}}^i - B(E2)_{\text{th}}^i)^2},$$

$$\Delta_2(E2) = \sqrt{\frac{1}{N_{E2}} \sum_i \left( \frac{B(E2)_{\text{ex}}^i - B(E2)_{\text{th}}^i}{B(E2)_{\text{ex}}^i} \right)^2}, \quad (4)$$

where the sums are over the available data points,  $N_E$  and  $N_{E2}$  in number, respectively. Note that the first rms deviation for the E2 data,  $\Delta_1(E2)$ , is rather insensitive to small E2 transitions while  $\Delta_2(E2)$  probably assigns too much weight to them. The rms deviations vary rather weakly except for small values of  $\chi$ , but both energies and E2 transitions are optimized for  $\chi \approx -0.20$ . This value of  $\chi$  and the parameters given in table 2 determine all spectra shown below.

In the above procedure care has been taken to undertake a gradual release of the parameters, instead of immediately attempting a full 11-parameter fit. This method has proven to be numerically stable but it offers no guarantee that the global minimum of the 11-dimensional parameter space will be reached, instead of a local one. Finding the global minimum is all the more problematic since some of the parameters, especially those that account for the fractional-filling dependence, offer little intuitive insight and are thus entirely unknown *a priori*. The character of the minimum corresponding to the parameters of table 2 has been checked by choosing different starting values for the  $x_{01}$  and  $x_{10}$  parameters, leading always to final parameter sets that are close to the one shown, within numerical errors. While this is not a proof of the global character of the minimum, it is a good indication of it.

The experimental and calculated energy spectra are compared in figures 1 and 2. The experimental energies are taken from the National Nuclear Data Center [18] with additional information concerning the nuclei  $^{108}\text{Pd}$  and  $^{112,118,120}\text{Pd}$  from the references [19, 20]. Some of the spin assignments are uncertain (brackets in NNDC); these are not shown on the figure to avoid overcrowding. In the even-even Mo, Ru and Pd isotopes with  $N \geq 52$ , all known levels of the ground-state, quasi- $\gamma$  and quasi- $\beta$  bands with angular momentum up to  $J = 10$  are considered in the fit while for Zr only

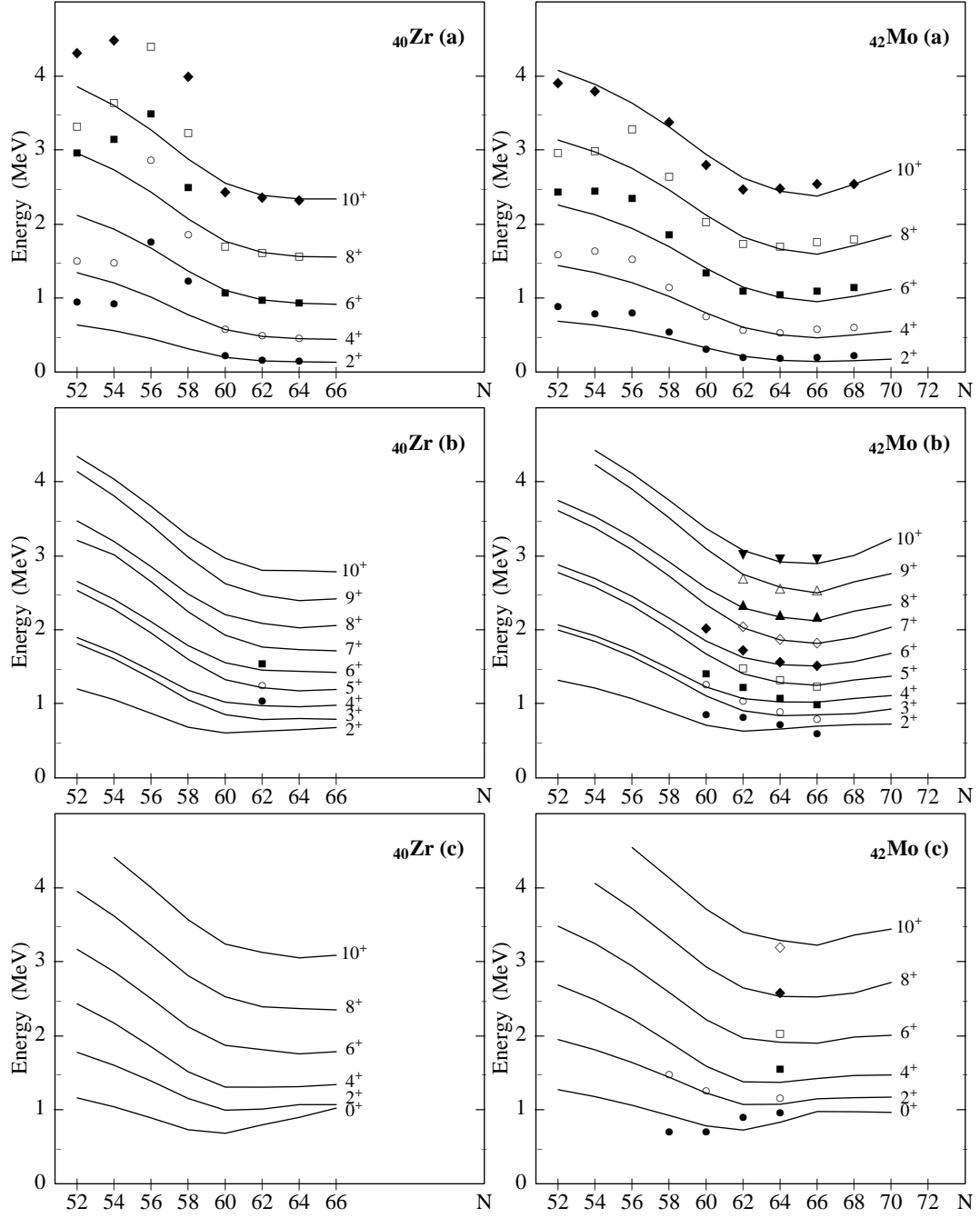


**Figure 1.** The experimental (symbols) and calculated (lines) energy spectra for the Zr isotopes with  $52 \leq N \leq 66$  (left) and the Mo isotopes with  $52 \leq N \leq 70$  (right): (a) ground-state, (b) quasi- $\gamma$  and (c) quasi- $\beta$  bands. Only levels in Zr isotopes with  $N \geq 60$  are fitted. All experimental levels shown for Mo are included in the fit.

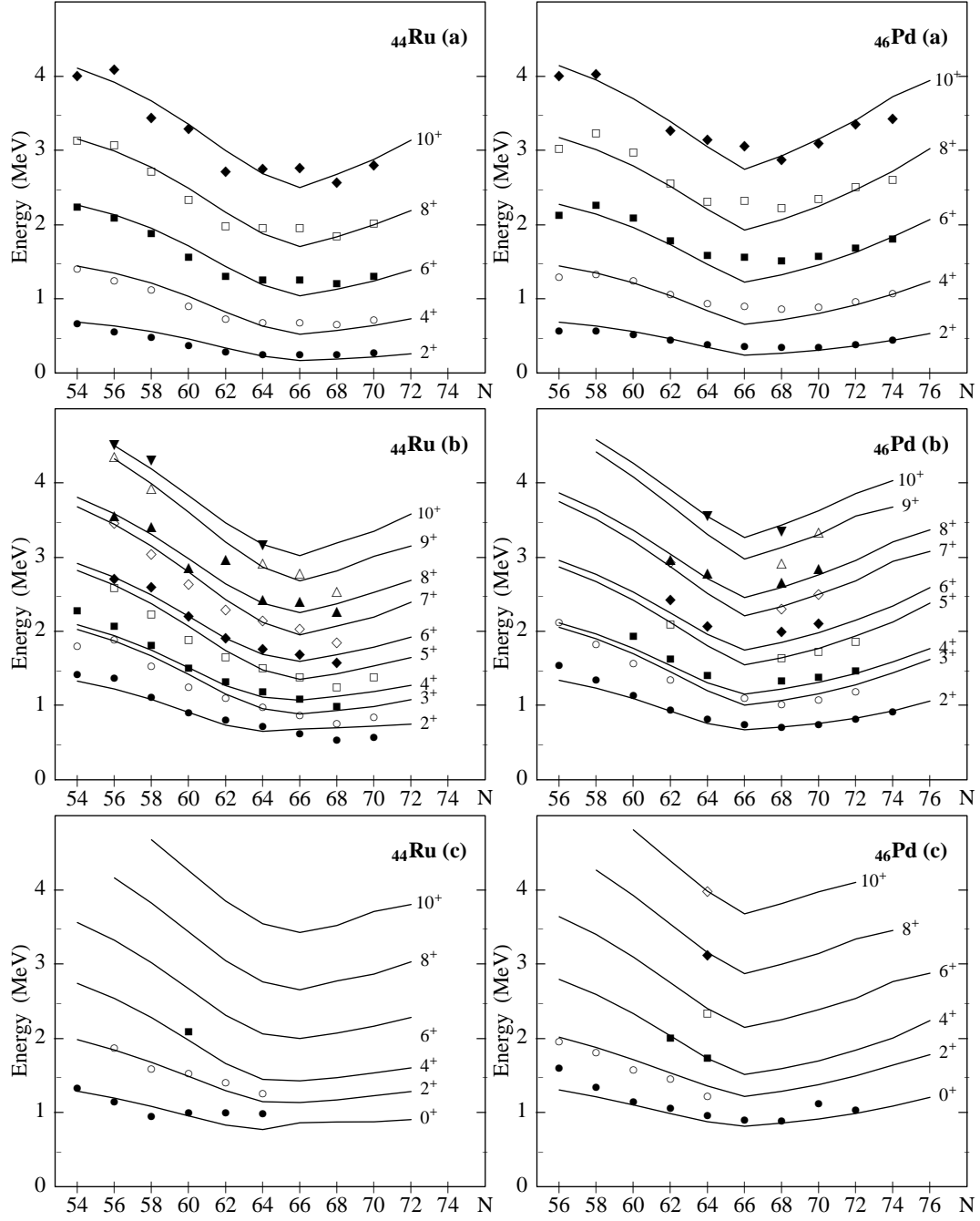


**Figure 2.** The experimental (symbols) and calculated (lines) energy spectra for the Ru isotopes with  $54 \leq N \leq 72$  (left) and for the Pd isotopes with  $56 \leq N \leq 76$  (right): (a) ground-state, (b) quasi- $\gamma$  and (c) quasi- $\beta$  bands. All experimental levels shown are included in the fit.

**Table 3.** Root-mean-square deviations  $\Delta(E)$  when Zr isotopes with neutron number  $N \geq N_0$  are included in the fit.

$N_0$	60	58	56	54	52
$\Delta(E)$ (keV)	120	158	214	215	217

isotopes with  $N \geq 60$  are included. Figure 1 nevertheless also shows the experimental levels for  $^{92-98}\text{Zr}$  (*not* included in the fit) merely to indicate that these strongly deviate from what is predicted from systematics. To give an illustration of the deviations, the  $2_1^+$  level in  $^{96}\text{Zr}$  is observed at 1751 keV while it is calculated at 444 keV. These differences are indicative of the closure of the  $1d_{5/2}$  shell at  $N = 56$ , resulting in a nearly doubly-magic behaviour of  $^{96}\text{Zr}$ . These considerations can be made quantitative by including the ground-state bands of some of the lighter Zr isotopes in the energy fit. As illustrated in table 3 even the inclusion of just one isotope,  $^{98}\text{Zr}$ , yields a dramatic increase in the rms deviation of the fit to the entire region. Effects of  $1d_{5/2}$  shell persist in  $^{100}\text{Zr}$  which exhibits a low-lying  $K^\pi = 0^+$  band at 331 keV. This clearly cannot be the collective first-excited  $K^\pi = 0^+$  band of the IBM-1 and therefore the band is not included in the fit. The next-excited  $K^\pi = 0^+$  band at 829 keV is possibly the quasi- $\beta$  band of the IBM-1, which is calculated at 682 keV.

We emphasize that the IBM-1 parametrization (3) depends on the counting of the number of *valence* nucleons and hence on the definition of shell closures and magic numbers. Since  $N = 56$  is not included as a magic number, it is therefore no surprise that the structural features associated with this shell closure are absent from the present calculations. The inclusion of *all* Zr isotopes in a successful fit would necessarily require a refined parametrization that takes account of the  $N = 56$  closure. However, even at the present level of approximation, we believe to have illustrated with this example that the unified fits of the type used here are sensitive to nuclear shell effects. This feature could be of use to detect precursor effects of shell closures in extrapolations toward unknown regions of the nuclear chart.

In the present application excluding Zr isotopes with  $N < 60$ , we arrive at a description of 335 collective levels in 31 nuclei with a rms deviation from the observed level energies of 120 keV. The most notable systematic discrepancies are found for (i) the spectra of  $N \sim 56$  Mo isotopes due to some remnant effect of the  $N = 56$  closure, (ii) the energy of the  $\gamma$  band in  $^{102}\text{Zr}$  which is predicted lower than it is observed, and (iii) some mid-shell nuclei like  $^{100}\text{Ru}$  and  $^{102}\text{Pd}$  which behave less collectively than predicted by IBM-1 systematics.

On the basis of the parametrization thus established it is now possible to make predictions for more exotic nuclei for which up to now no spectroscopic information is available. This is illustrated in figures 1 and 2 where systematically the predictions for the next (unknown) even-even isotopes are shown, that is, for  $^{106}\text{Zr}$ ,  $^{112}\text{Mo}$ ,  $^{116}\text{Ru}$  and  $^{122}\text{Pd}$ . Clearly, predictions further away from stability are possible as well but become



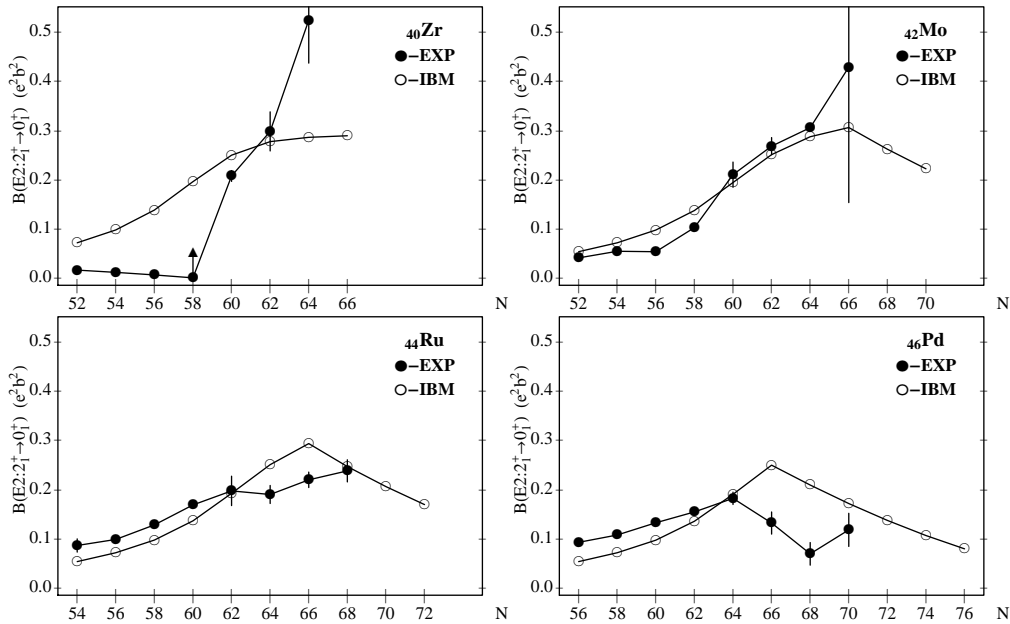


**Figure 3.** The experimental (full symbols) and calculated (open symbols)  $B(E2; 2_1^+ \rightarrow 0_1^+)$  values in the Zr, Mo, Ru and Pd isotopes.

increasingly uncertain.

Once the wave functions of all states have been determined in this unified fit, one can also calculate the E2 transition rates with an overall effective charge  $e_b = 0.097\text{ eb}$ , adjusted to reproduce the  $2_1^+ \rightarrow 0_1^+$  and  $4_1^+ \rightarrow 2_1^+$  transitions. The results for the  $B(E2; 2_1^+ \rightarrow 0_1^+)$  and  $B(E2; 4_1^+ \rightarrow 2_1^+)$  values are shown in figures 3 and 4, respectively. These are a measure of the collective behaviour of the nucleus and our calculation generally follows the observed trends. A glaring exception to this overall agreement is the  $2_1^+ \rightarrow 0_1^+$  transition in the Zr isotopes with  $N < 60$  where the observed  $B(E2)$  value is only fraction from what is expected from systematics. This again is due to the neglect in the calculation of the  $1d_{5/2}$  closure at  $N = 56$ . There is also a mid-shell mismatch for the Pd isotopes which is calculated at  $N = 66$  but observed at  $N = 64$ . Figure 5 shows the  $B(E2; 0_2^+ \rightarrow 2_1^+)$  values. In the vibrational  $U(5)$  limit this transition corresponds to one from a two-phonon to a one-phonon state which is allowed while in the more deformed limits  $SO(6)$  and  $SU(3)$  this  $B(E2)$  value is much smaller. This argument gives a qualitative understanding of the theoretical results shown in figure 5.

As a further illustration of the kind of accuracy obtained for the  $B(E2)$  values in this overall fit, we show in table 4 the results for three nuclei,  $^{100}\text{Ru}$ ,  $^{104}\text{Pd}$  and  $^{108}\text{Pd}$ , for which extensive E2 data is known.

The geometric character of all nuclei can be visualized by plotting the potential energy surface  $V(\beta, \gamma)$  obtained from the IBM-1 Hamiltonian in the classical limit [21,

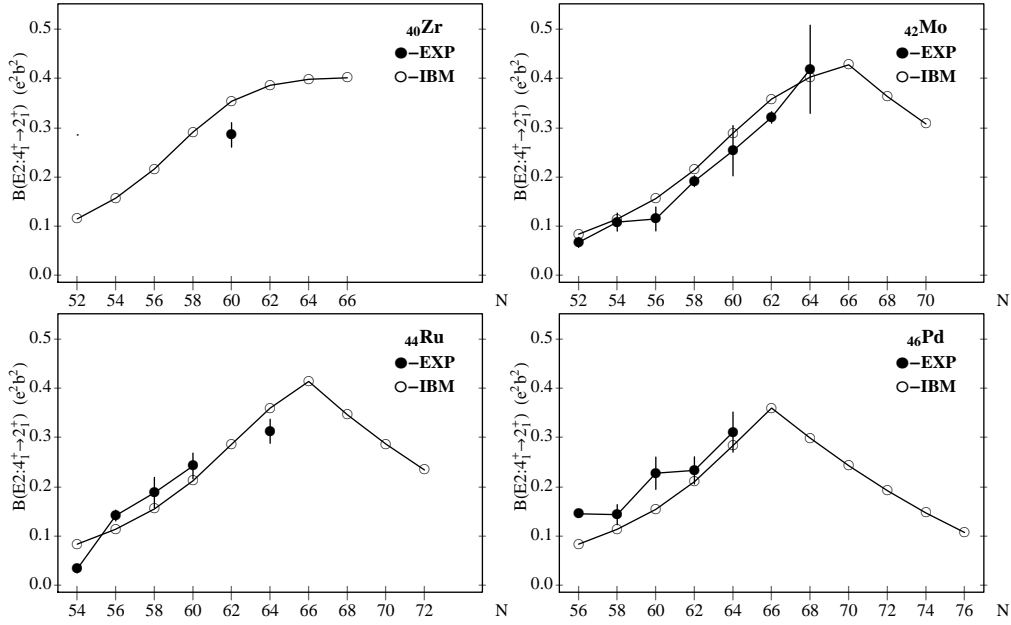


**Figure 4.** The experimental (full symbols) and calculated (open symbols)  $B(E2; 4_1^+ \rightarrow 2_1^+)$  values in the Zr, Mo, Ru and Pd isotopes.

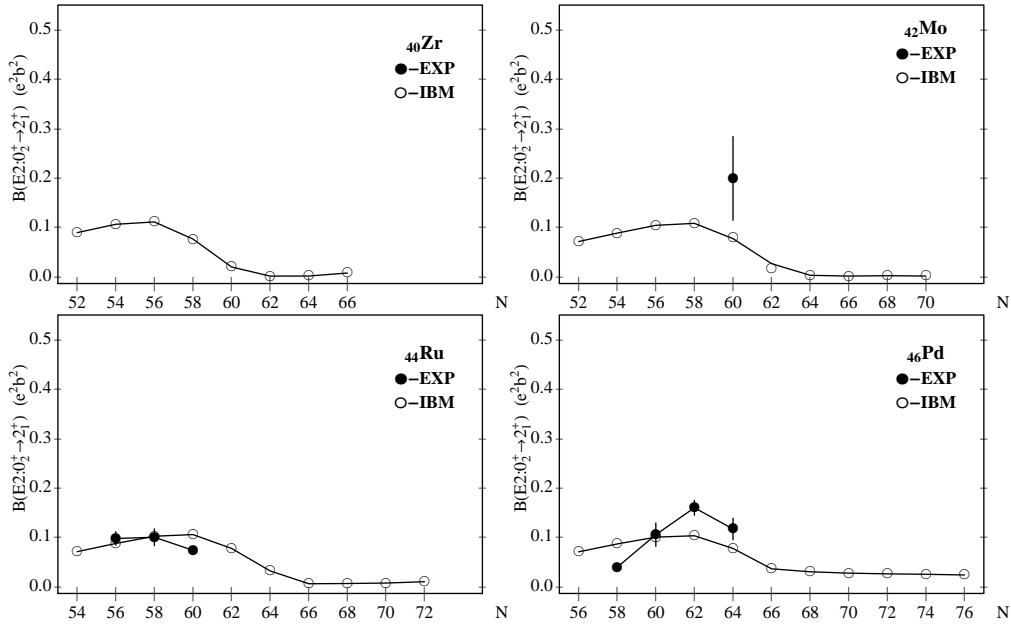


**Figure 5.** The experimental (full symbols) and calculated (open symbols)  $B(E2; 0_2^+ \rightarrow 2_1^+)$  values in the Zr, Mo, Ru and Pd isotopes.

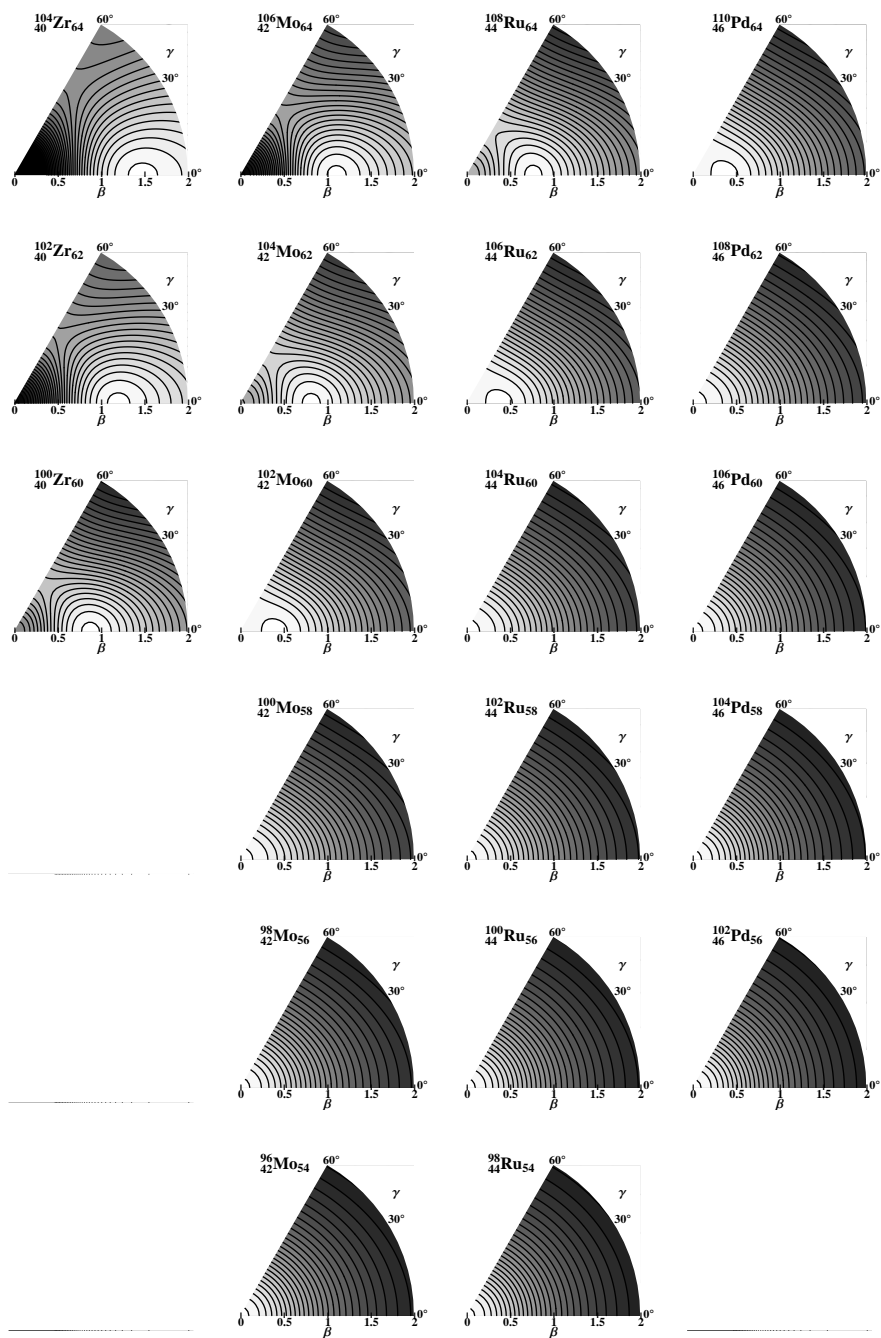


**Figure 6.** Potential energy surfaces for all nuclei (first part).

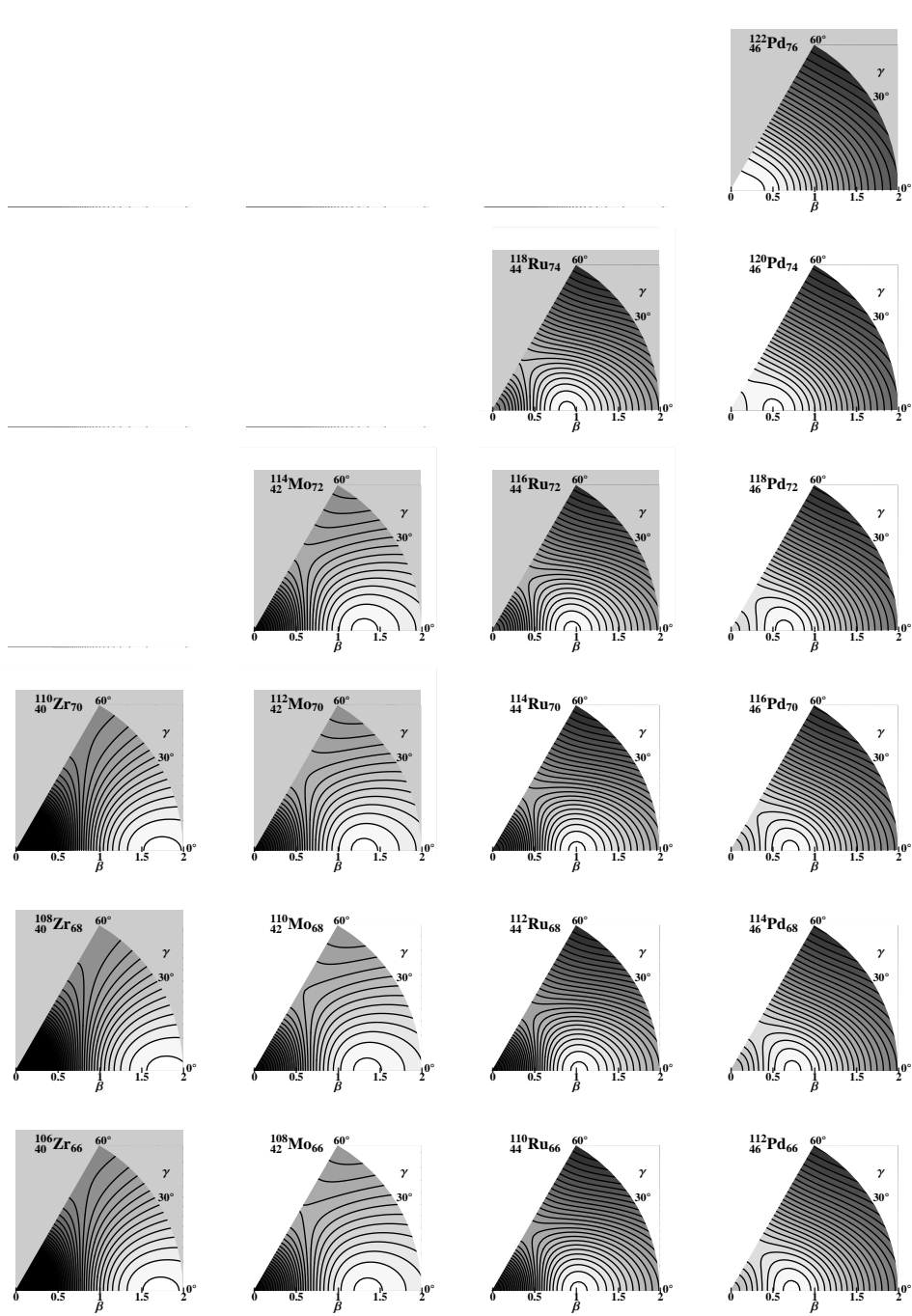


**Figure 7.** Potential energy surfaces for all nuclei (second part). The grey background indicates a potential surface for a predicted nucleus.

**Table 4.** Experimental and calculated  $B(E2; J_i^\pi \rightarrow J_f^\pi)$  values in units of  $10^2 \text{ e}^2\text{fm}^4$  in  $^{100}\text{Ru}$ ,  $^{104}\text{Pd}$  and  $^{108}\text{Pd}$ .

$J_i^\pi \rightarrow J_f^\pi$	$^{100}\text{Ru}$		$^{104}\text{Pd}$		$^{108}\text{Pd}$	
	Expt	IBM-1	Expt	IBM-1	Expt	IBM-1
$2_1^+ \rightarrow 0_1^+$	9.8 (0.1)	7.1	11 (0.6)	7.1	15 (0.5)	14
$4_1^+ \rightarrow 2_1^+$	14 (1.1)	11	14 (2)	11	23 (2.8)	21
$6_1^+ \rightarrow 4_1^+$	< 47	13	—	13	33 (3.4)	24
$8_1^+ \rightarrow 6_1^+$	—	12	—	12	45 (6.1)	25
$0_2^+ \rightarrow 2_1^+$	9.7 (1.4)	8.6	3.8 (0.4)	8.5	16 (1.5)	10
$2_2^+ \rightarrow 0_1^+$	$0.52^{(+0.11)}_{(-0.14)}$	0.004	0.38 (0.03)	0.004	0.25 (0.02)	0.10
$2_2^+ \rightarrow 2_1^+$	8.5 (0.11)	11	6.3 (4.9)	11	22 (1.5)	19
$4_2^+ \rightarrow 2_1^+$	$0.52^{(+0.22)}_{(-0.06)}$	0.003	0.17 (0.17)	0.003	0.04 (0.04)	0.04
$4_2^+ \rightarrow 2_2^+$	—	6.7	7.3 (7.3)	6.7	17 (1.8)	12
$4_2^+ \rightarrow 4_1^+$	7.4 (4.7)	6.0	2.9 (2.9)	6.0	9.2 (1.8)	10

22, 23]. The classical limit of the IBM-1 Hamiltonian (1) is

$$V(\beta, \gamma) = \frac{N}{1 + \beta^2} \left( a_{00}^{(1)} + a_{10}^{(1)} \beta^2 \right) + \frac{N(N-1)}{(1 + \beta^2)^2} \left( a_{00}^{(2)} + a_{10}^{(2)} \beta^2 + a_{01}^{(2)} \beta^3 \cos 3\gamma + a_{20}^{(2)} \beta^4 \right), \quad (5)$$

where the coefficients  $a_{kl}^{(n)}$  are given by

$$\begin{aligned} a_{00}^{(1)} &= 5\kappa, & a_{10}^{(1)} &= \epsilon + (1 + \chi^2)\kappa + 6\kappa' + \lambda, & a_{00}^{(2)} &= \frac{1}{4}\kappa'', \\ a_{10}^{(2)} &= 4\kappa - \frac{1}{2}\kappa'', & a_{01}^{(2)} &= -4\sqrt{\frac{2}{7}}\chi\kappa, & a_{20}^{(2)} &= \frac{2}{7}\chi^2\kappa + \frac{1}{4}\kappa'' + \lambda. \end{aligned} \quad (6)$$

Since the parameters in this potential depend on the fractional fillings of the valence shells, we arrive at a geometry for each nucleus which changes with neutron and proton numbers and which has been obtained in an unbiased and straightforward way from the observed excitation spectra. This is illustrated in figures 6 and 7, where the potentials are shown for all nuclei included in the fit as well as for some which are predicted. For the sake of a correct interpretation of these potential surfaces, we recall that  $\gamma$  is identical to the corresponding parameter in the Bohr–Mottelson geometric model [24] while  $\beta$  is only proportional to it, the proportionality factor depending on the ratio of the valence over the total nucleon numbers [25]. The potential energy surface of the nucleus  $^{108}\text{Ru}$  has recently been calculated in variety of ways. Möller *et al.* [26] showed that deviations from axial symmetry can be important and, in the specific case of  $^{108}\text{Ru}$ , obtained a potential energy surface with triaxial minimum. With the simple parametrization of the IBM-1 Hamiltonian as proposed here which is limited to two-body interactions, no triaxial minimum can be obtained [27], a result confirmed by the surfaces shown in figures 6 and 7. It is also seen, however, that the specific potential for  $^{108}\text{Ru}$  is rather soft in  $\gamma$ . Triaxial minima can be obtained when cubic terms are added to the IBM-1 Hamiltonian [28, 29]. In comparison with the results obtained in reference [29] for the

nuclei  $^{108,110,112}\text{Ru}$ , we observe that the potential surfaces shown here show less variation with neutron number since they are derived from a global fit to many nuclei while in the former study the fits were carried out nucleus by nucleus. Also shown in figures 6 and 7 are the potential energy surfaces for the predicted neutron-rich nuclei. As can be seen from the figures, their geometry varies from strongly deformed in the neutron-rich Zr isotopes to spherical in  $^{122}\text{Pd}$ .

#### 4. Conclusions

We have suggested in this paper the use of IBM-1 for global calculations of large regions of the nuclear chart and have illustrated the idea with an application to the  $A \sim 100$  region. The present work calls for several features to be studied in more detail. The first concerns the technical issue of finding the set of parameters that corresponds to the *global* minimum of the rms deviation. The minimization algorithm that has been used here is a straightforward linearization procedure of the eigenvalue problem associated with the Hamiltonian (1) which has no trouble in finding a *local* minimum. We have found no dependence of the converged parameters on various choices of their initial values but it would be of interest to confirm the global character of the minimum using a different algorithm which samples large parameter regions. Secondly, the dependence of the parameters on the fractional fillings  $f_\rho$  of the valence neutron and proton shells requires further study. We have proposed here a dependence on  $n_\rho/\Omega_\rho$  but other choices should be investigated as well, such as a dependence on  $N_\rho/\Omega_\rho$  (where  $N_\rho$  is the boson number) or on Casten's factor  $P = N_\nu N_\pi / (N_\nu + N_\pi)$  [12]. Furthermore, a possible dependence on subshells must also be studied. A proper treatment of these effects and their dependence on valence nucleon number must draw inspiration from the microscopic foundation of the IBM. For example, in this study we have taken a constant value of  $\chi$ , the parameter appearing in the quadrupole operator. This is possibly a reasonable approximation for the restricted set of nuclei considered here but it will certainly be inadequate if large regions of the nuclear chart are fitted simultaneously. This inadequacy might be satisfactorily resolved by a proper estimate of this parameter based on the shell-model interpretation of the IBM. An alternative strategy is to adopt a functional dependence of  $\chi$  on valence-particle number suggested by microscopy, containing a few parameters that are fitted to the data. Finally, we point out that the type of calculation described here opens up the possibility for a simultaneous and global treatment of nuclear ground-state properties (such as masses and radii) in addition to the excited-state properties discussed in this paper. A possible strategy for merging the calculations of ground- and excited-state energies in the framework of the interacting boson model was outlined in reference [30] with preliminary results for even-even nuclei in the major shell with  $82 < N < 126$  and  $50 < Z < 82$  but further investigations of this approach are required.

## Acknowledgements

This work was supported by the Scientific and Technological Research Council of Turkey (TUBITAK) under project nr 107T557, and by the Agence Nationale de Recherche, France, under contract nr ANR-07-BLAN-0256-03.

## 5. References

- [1] Bender M, Heenen P-H and Reinhard P-G 2003 *Rev. Mod. Phys.* **75** 121
- [2] Caurier E, Martínez-Pinedo G, Nowacki F, Poves A and Zuker A P 2005 *Rev. Mod. Phys.* **77** 427
- [3] Arima A and Iachello F 1976 *Ann. Phys. (N.Y.)* **99** 253
- [4] Arima A and Iachello F 1978 *Ann. Phys. (N.Y.)* **111** 201
- [5] Arima A and Iachello F 1979 *Ann. Phys. (N.Y.)* **123** 468
- [6] Arima A, Otsuka T, Iachello F and Talmi I 1977 *Phys. Lett. B* **66** 205
- [7] Otsuka T, Arima A and Iachello F 1978 *Nucl. Phys. A* **309** 1
- [8] Iachello F and Arima A 1987 *The Interacting Boson Model* (Cambridge: Cambridge University Press)
- [9] Gómez A, Castaños O and Frank A 1995 *Nucl. Phys. A* **589** 267
- [10] Lalkowski S and Van Isacker P 2009 *Phys. Rev. C* **79** 044307
- [11] Casten R F, Frank W and von Brentano P 1985 *Nucl. Phys. A* **444** 133
- [12] Casten R F 1985 *Nucl. Phys. A* **443** 1
- [13] Nomura K, Shimizu N and Otsuka T 2008 *Phys. Rev. Lett.* **101** 142501
- [14] Büyükatana M, Van Isacker P and Uluer İ 2008 *AIP Conf. Proc.* **1072** 223
- [15] Büyükatana M and Uluer İ 2010 *AIP Conf. Proc.* **1231** 201
- [16] Pan X-W, Otsuka T, Chen J-Q and Arima A 1992 *Phys. Lett. B* **287** 1
- [17] Warner D D and Casten R F 1982 *Phys. Rev. Lett.* **48** 1385
- [18] National Nuclear Data Center (NNDC) <http://www.nndc.bnl.gov/>
- [19] Alcántara-Núñez J A, Oliveira J R B, Cybulska E W, Medina N H, Rao M N, Ribas R V, Rizzutto M A, Seale W A, Falla-Sotela F and Wiedemann K T 2005 *Phys. Rev. C* **71** 054315
- [20] Stoyer M A *et al* 2007 *Nucl. Phys. A* **787** 455c
- [21] Ginocchio J N and Kirson M W 1980 *Phys. Rev. Lett.* **44** 1744
- [22] Dieperink A E L, Scholten O and Iachello F 1980 *Phys. Rev. Lett.* **44** 1747
- [23] Bohr A and Mottelson B R 1980 *Phys. Scripta* **22** 468
- [24] Bohr A and Mottelson B R 1975 *Nuclear Structure. II Nuclear Deformations* (Benjamin: New York)
- [25] Ginocchio J N and Kirson M W 1980 *Nucl. Phys. A* **350** 31
- [26] Möller P, Bengtsson R, Carlsson B G, Olivius P and Ichikawa T 2006 *Phys. Rev. Lett.* **97** 162502
- [27] Van Isacker P and Chen J-Q 1981 *Phys. Rev. C* **24** 684
- [28] Stefanescu I, Gelberg A, Jolie J, Van Isacker P, von Brentano P, Luo Y X, Zhu S J, Rasmussen J O, Hamilton J H, Ramayya A V and Che X L 2007 *Nucl. Phys. A* **789** 125
- [29] Sorgunlu B and Van Isacker P 2008 *Nucl. Phys. A* **808** 27
- [30] Van Isacker P 2009 *Rev. Mex. Fís.* **55** (2) 66